

AD-A063 822

VISIDYNE INC BURLINGTON MASS
IR BACKGROUND SUPPRESSION STUDIES, (U)

F/G 20/6

UNCLASSIFIED

MAY 77 O SHEPHERD, W P REIDY, T F ZEHNPFENNIG F19628-76-C-0198
SCIENTIFIC-1 AFGL-TR-77-0277 NL

| OF |

AD
A063 822



END
DATE
FILMED
3-79
DDC

LEVEL II

13
B

AD A063822

DDC FILE COPY

18 AFGL TR-77-0277

6 IR BACKGROUND SUPPRESSION STUDIES,

10 C./Shepherd,
W.P./Reidy,
T.F./Zehnpfennig,
G.A./Vanasse
A.T./Stair, Jr

Visidyne, Inc.
19 Third Avenue
Northwest Industrial Park
Burlington, Massachusetts 01803

DDC
RECEIVED
JAN 26 1979
C

11 15 May 1977

12 39P.

14 SCIENTIFIC [REDACTED] -1

16 2310
ILIR

17 G4,6K

15 Approved for public release; distribution unlimited.
F19628-76-C-0198

This research was supported by the Air Force In-House
Laboratory Independent Research Fund

AIR FORCE GEOPHYSICS LABORATORY
AIR FORCE SYSTEMS COMMAND
UNITED STATES AIR FORCE
HANSCOM AFB, MASSACHUSETTS 01731

390 862
79 01 26 012

Qualified requestors may obtain additional copies from the Defense Documentation Center. All others should apply to the National Technical Information Service.

Unclassified

SECURITY CLASSIFICATION OF THIS PAGE (When Data Entered)

REPORT DOCUMENTATION PAGE		READ INSTRUCTIONS BEFORE COMPLETING FORM
1. REPORT NUMBER AFGL-TR-77-0277 ✓	2. GOVT ACCESSION NO.	3. RECIPIENT'S CATALOG NUMBER
4. TITLE (and Subtitle) IR BACKGROUND SUPPRESSION STUDIES		5. TYPE OF REPORT & PERIOD COVERED Scientific Report No. 1 ✓
		6. PERFORMING ORG. REPORT NUMBER
7. AUTHOR(s) O. Shepherd G.A. Vanasse* T.F. Zehnpfennig A.T. Stair, Jr.* W.P. Reidy		8. CONTRACT OR GRANT NUMBER(s) F19628-76-C-0198 ✓
9. PERFORMING ORGANIZATION NAME AND ADDRESS Visidyne, Inc. ✓ 19 Third Avenue, Northwest Industrial Park Burlington, Massachusetts 01803		10. PROGRAM ELEMENT, PROJECT, TASK AREA & WORK UNIT NUMBERS 61102F 2310G4AF ILIR
11. CONTROLLING OFFICE NAME AND ADDRESS Air Force Geophysics Laboratory Hanscom AFB, Massachusetts 01731 Monitor/J.A. Sandock/OPR		12. REPORT DATE 15 May 1977
		13. NUMBER OF PAGES 39
14. MONITORING AGENCY NAME & ADDRESS (if different from Controlling Office)		15. SECURITY CLASS. (of this report) Unclassified
		15a. DECLASSIFICATION/DOWNGRADING SCHEDULE
16. DISTRIBUTION STATEMENT (of this Report) Approved for public release; distribution unlimited.		
17. DISTRIBUTION STATEMENT (of the abstract entered in Block 20, if different from Report)		
18. SUPPLEMENTARY NOTES * Hanscom AFB, MA 01731 This research was supported by the Air Force In-House Laboratory Independent Research Fund		
19. KEY WORDS (Continue on reverse side if necessary and identify by block number) Background Interferometry Suppression		
20. ABSTRACT (Continue on reverse side if necessary and identify by block number) A brief description of the background suppression scheme is described, and results obtained using the defocussing technique, which is a Visidyne proprietary implementation of the scheme, are presented. It has been demonstrated that a background suppression ratio of two orders of magnitudes can be obtained.		

DD FORM 1 JAN 73 1473

EDITION OF 1 NOV 65 IS OBSOLETE

Unclassified

SECURITY CLASSIFICATION OF THIS PAGE (When Data Entered)

79 01 26 012

UNCLASSIFIED

SECURITY CLASSIFICATION OF THIS PAGE(When Data Entered)



UNCLASSIFIED

SECURITY CLASSIFICATION OF THIS PAGE(When Data Entered)

TABLE OF CONTENTS

	PAGE
1. INTRODUCTION	6
2. PRINCIPLE OF BOSS TECHNIQUE	6
3. CONCEPTUAL IMPLEMENTATIONS	17
4. PROBLEM OF NON-UNIFORM BACKGROUND	25
5. ADVANTAGES OF THE TECHNIQUE	25
6. OTHER CAPABILITIES	27
7. LABORATORY MEASUREMENTS OF BACKGROUND SUPPRESSION	28
8. LABORATORY MEASUREMENTS OF BACKGROUND SUPPRESSION WITH OCCULATION	33
9. LABORATORY MEASUREMENTS OPTICAL TARGET FILTERING	33
10. PRESENT STATUS AND FUTURE WORK	39

ADDRESS FOR

NAME _____

PO BOX _____

CITY/STATE/ZIP _____

PHONE NUMBER _____

BY _____

DISTRIBUTION/AVAILABILITY CODES

Date _____ OF CIRC.

A

FOREWORD

The experimental demonstration reported herein was performed using AFGL Laboratory Director's Funds under Project ILIR-6K. The research involved is based on the following pending patents:

Double-Beaming in Fourier Spectroscopy
G. Vanasse, AFGL

Background Suppression-Surveillance Technique
R. Murphy, G. Vanasse, and A.T. Stair, Jr., AFGL

Method of and Apparatus for Background Suppression in
Interferometric Analysis, VI-112J
T. Zehnpfennig, Visidyne, Inc.

IR BACKGROUND SUPPRESSION STUDIES

1. INTRODUCTION

In this report we will give a description of the basic idea of the AFGL background optical suppression scheme (BOSS) starting from basic principles. The potential advantages of the technique will be pointed out and various schemes for implementing the technique will be illustrated. Results obtained during the duration of the effort to demonstrate the technique (work which was funded by the AFGL Laboratory Director's Fund) will be presented.

2. PRINCIPLE OF BOSS TECHNIQUE

The essence of the technique^{1,2} is to use some type of interferometer (Michelson or one of its variations) into which two beams are directed, and also make use of the two beams which exit from the instrument. This section will describe implementations of such a system and present reasons for wanting to use such a system, as well as the obvious advantages (over a single input, single output beam system) that such a system yields.

First of all, since we use an interferometer, we automatically have the well-known throughput^{3} advantage inherent to interferometers. Also, if the system is to be used in an "optical path difference scanning" mode, or in a fixed retardation mode, with jittering, we have the other well-known advantage of Fourier spectroscopy called the multiplex advantage^{3}. Another advantage of the interferometer is its large free spectral range which is of importance for determining the spectral features of targets and backgrounds over broad spectral regions.

All of the above advantages of interferometers are well known, have been described many times in the literature, and will not be dealt with here. The only reason for their being mentioned is that the heart of the

system for BOSS is an instrument which already enjoys the above-mentioned advantages of the interferometer even before we adapt it for the AFGL background suppression scheme.

Let us consider the two Michelson interferometers illustrated in Fig. 1 and their corresponding outputs illustrated to their right. In the upper left corner of the figure, radiation enters the interferometer at IN and strikes the upper face of the dielectric beamsplitter B.S. The radiation is divided at the beamsplitter and ideally half the light travels through the beamsplitter to be reflected back to the beamsplitter by mirror M1. The other half of the light is reflected by the beam splitter and again reflected back to the beamsplitter by mirror M2. The two beams are thus recombined at the beamsplitter where part of the radiation is transmitted to the detector, D, and part is reflected in the direction of the incoming beam. If the mirror M1 is moved at a constant speed v , when monochromatic radiation of wavelength $\lambda = 1/\sigma$ (cm^{-1}) enters the interferometer, the detector output will be a sinusoidal function of electrical frequency f given by $f_\sigma = 2 v\sigma$; the factor of 2 occurring because the optical path difference in the interferometer is twice the displacement of mirror M1. For radiation of broad spectral distribution $B(\sigma)$, the detector output as a function of path difference x in the interferometer will look like the curve at the upper right of Fig. 1. The functional character of the upper curve D_μ (or the detector output $D_\mu(x)$) as a function of path difference x is given by

$$D_\mu(x) = \int_{\sigma_1}^{\sigma_2} B(\sigma) \left[\frac{1}{2} + \frac{1}{2} \cos 2\pi\sigma x \right] d\sigma \quad (1)$$

where the limits to the integral indicate the bandwidth $\Delta\sigma = (\sigma_2 - \sigma_1)$ of the radiation being studied; these limits will be dropped in the following equations.

We can rewrite Equation (1) as

$$D_\mu(x) - \frac{1}{2} \int B(\sigma) d\sigma = F_\mu(x) \quad (2)$$

where the function $F_\mu(x)$ is usually called the interferogram in Fourier

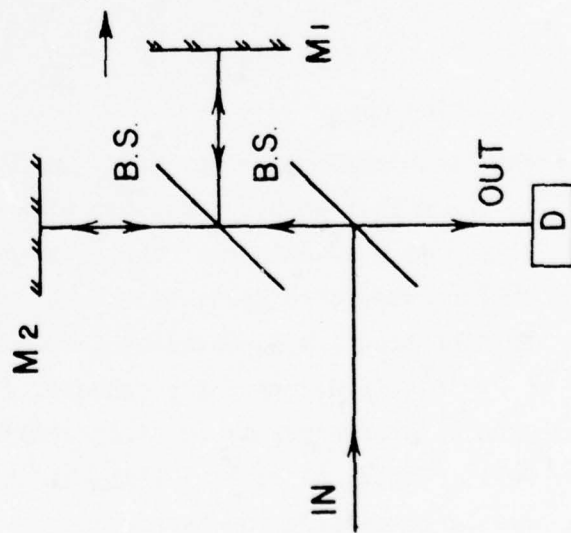
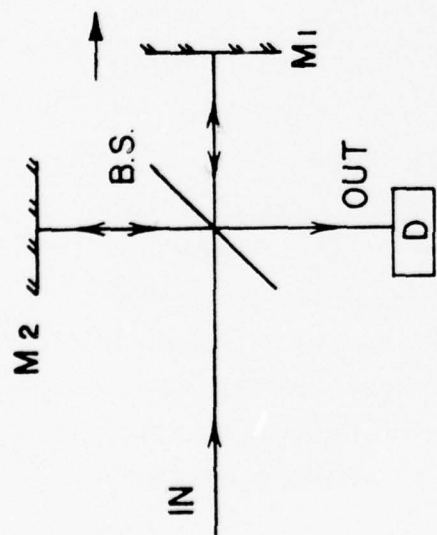
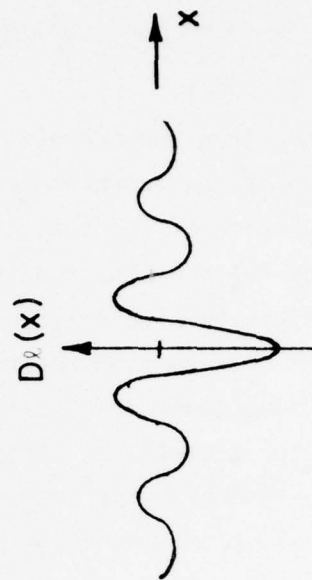
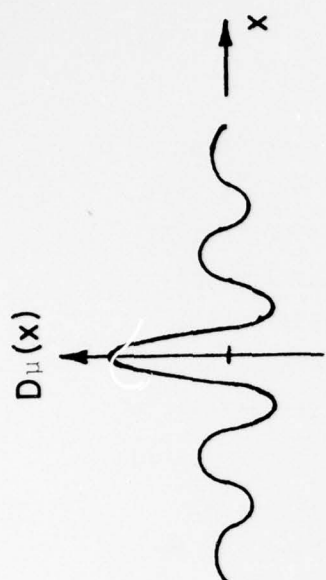


FIGURE 1

spectroscopy and is given by

$$F_{\mu}(x) = \frac{1}{2} \int B(\sigma) \cos 2\pi\sigma x d\sigma. \quad (3)$$

In essence then the curve at the upper right of Figure 1, the transmitted radiation, is the interferogram generated by the interferometer at the left when radiation of spectral distribution $B(\sigma)$ enters it. We notice that at $x = 0$ (no retardation) the interferogram has its peak value; that is, all the energy (assuming no losses) entering the interferometer falls on the detector. For another retardation not all of the radiation reaches the detector, some goes back toward the source. In fact, the transmitted radiation which goes to the detector is complementary to the reflected radiation which goes back to the source. Since they are complementary their sum should add up to a constant which equals the total energy entering the interferometer; which is what it should be from a consideration of the conservation of energy principle.

If now we consider what happens with the interferometer configuration at the lower left of Figure 1, we notice that the incoming beam strikes the lower face of the main interferometer beamsplitter, and everything goes on as with the previous configuration. The difference, of course, is that the transmitted beam (the one reaching the detector) produces the lower curve at the right of it which has the functional relation given by

$$D_{\ell}(x) = \int \left[\frac{1}{2} B(\sigma) - \frac{1}{2} B(\sigma) \cos 2\pi\sigma x \right] d\sigma, \quad (4)$$

and is complementary to the curve $D_{\mu}(x)$ above it in the figure.

Now that we have finished with the fundamentals we shall describe how we can take advantage of the complementary characteristics of the interferometer outputs to devise a concept for detecting a target which may be much fainter than its surrounding medium, or its background and/or foreground.

In simple terms, the concept is to somehow obtain complementary background interferograms so as to obtain a constant (or zero for dual output mode) electrical output; that is, an interferogram which has no modulation due to the disturbing background.

It should be indicated that in Figure 1 an extra beamsplitter was necessary in order to get the input beam to strike the lower face of the main beamsplitter. This particular configuration introduces losses and even more so if it were modified we are to go to a dual-output system as well. Consequently, to further describe our concept we shall use an interferometer configuration which produces physically separated input beams without extra beamsplitters and also physically separated output beams. We are now ready to describe the AFGL concept for enhanced target detection or discrimination by means of a background suppression technique.

Figure 2 illustrates an interferometer configuration where two input beams are physically separated by using just one extra mirror and no extra beamsplitter. The mirrors M1 and M2 have been replaced either by roof mirrors or cube-corner retroreflectors; cat's eye retroreflectors would probably be better. As shown in the upper drawing, the background radiation is made to enter as one beam B_μ striking the upper face of the beamsplitter, and as another beam B_ℓ striking the lower face of the beamsplitter. We can consider these beams as coming from adjacent fields-of-view of a somewhat uniform background. From what we have shown above, (as the mirror assembly M1 is moved) the beam B_μ by itself would produce a detector output given by

$$D_\mu(x) = \int \frac{1}{2} B(\sigma) [1 + \cos 2\pi\sigma x] d\sigma. \quad (5)$$

On the other hand, the lower beam B_ℓ itself would produce a detector output which would be

$$D_\ell(x) = \int \frac{1}{2} B(\sigma) [1 - \cos 2\pi\sigma x] d\sigma. \quad (6)$$

However, if we allow both background beams to enter the interferogram simultaneously, the detector output would be the sum D_s of $D_\mu(x) + D_\ell(x)$, namely

$$D_s(x) = \int B(\sigma) d\sigma, \quad (7)$$

which is a constant independent of path difference x as is shown in the upper right-hand trace of Figure 2. Suppose now that a target appears in the upper

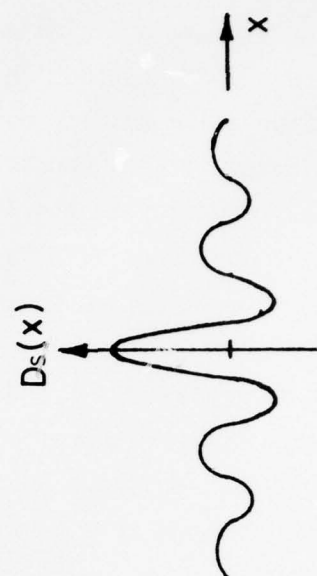
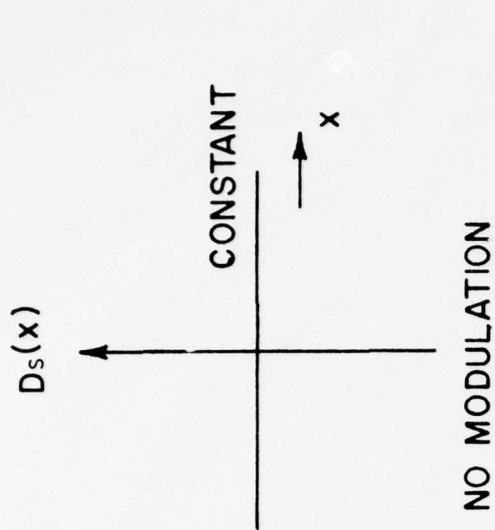
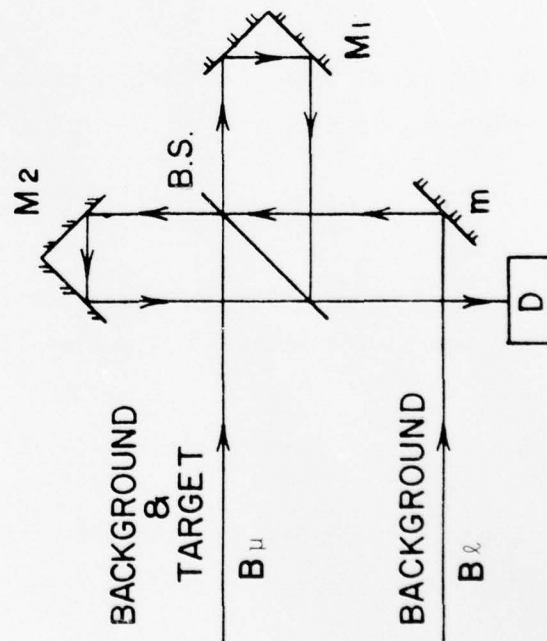
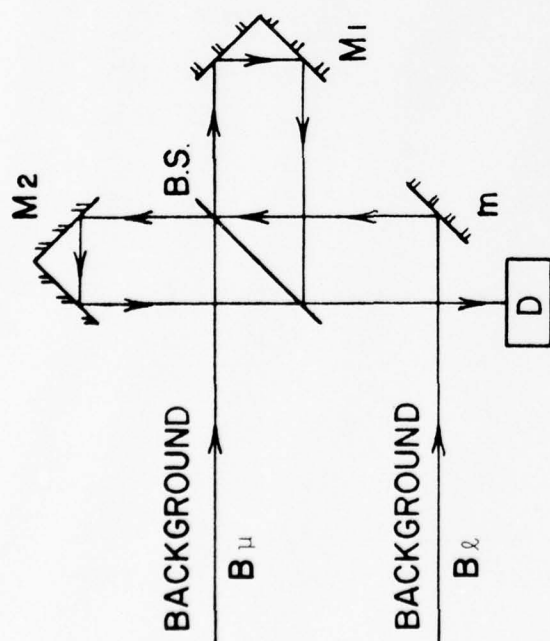


FIGURE 2

beam as shown in the lower left drawing in Figure 2. The two background beams will still yield a constant, but now there will appear modulation which will be due to the target radiation only.

With the configuration of Figure 2, we see that the background contribution is a constant output, namely

$$D_s = \int B(\sigma) d\sigma. \quad (8)$$

However, it is possible that the background intensity changes with time, or that the intervening medium produces intensity fluctuations, like scintillation. Although these occur in both beams, their fluctuations occur in phase and will cause D_s to be modulated according to these fluctuations, and would appear as a contribution to the modulation due to the target. To overcome this limitation the BOSS technique makes use of two output beams as discussed below.

Figure 3 shows the retroreflector interferometer equipped to use the two output beams. In the upper left drawing the upper beam B_u strikes the upper face of the beamsplitter, travels on through the interferometer as before, but now use is made of the beam that would go back toward the source, and it is made to fall on the detector D' . Detector D looks at the usual transmitted beam. Again, we see from the corresponding traces on the right that $D(x)$ and $D'(x)$ are complementary. The bottom half of Figure 3 illustrates a similar thing for the beam striking the lower face of the beamsplitter. But again, as before, a change of background intensity (or scintillation) affects both beams the same way as in Fig. 4; i.e., if scintillation causes $D(x)$ to increase by ϵ , it will also $D'(x)$ to increase by ϵ . Consequently, each detector will produce a signal given by

$$D'(x) + \epsilon(t) \text{ and } D(x) + \epsilon(t). \quad (9)$$

The solution for overcoming background temporal changes (or scintillation) is to difference the electrical outputs of the detectors and in that way obtain a zero signal (and not only a constant) for the background even when it is changing with time.

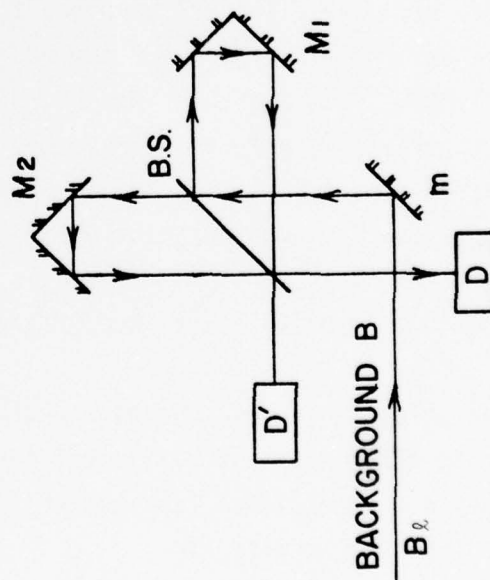
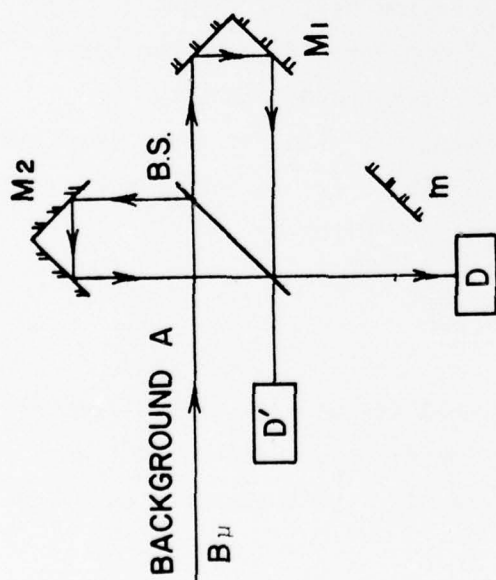
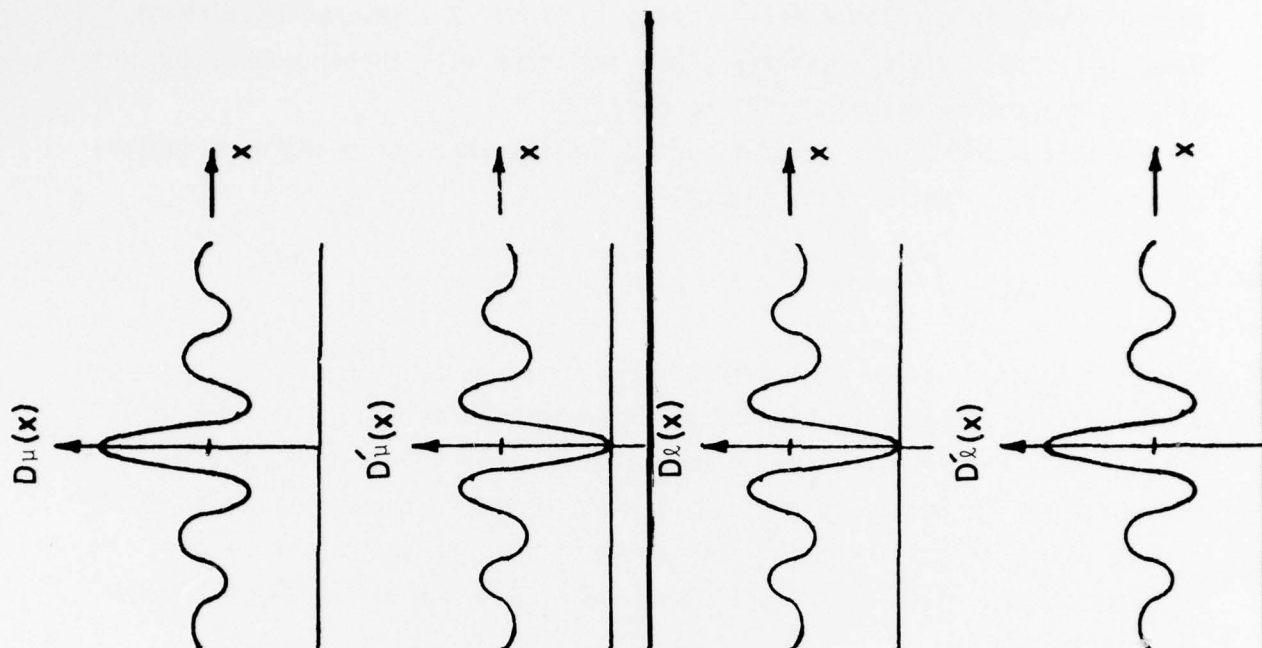


FIGURE 3

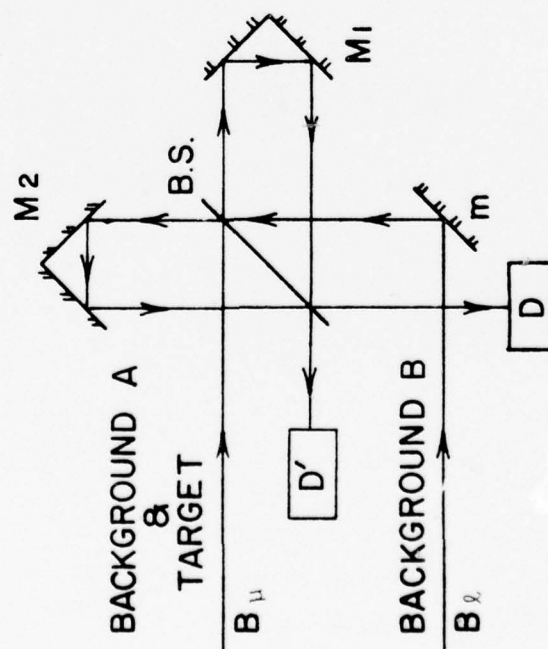
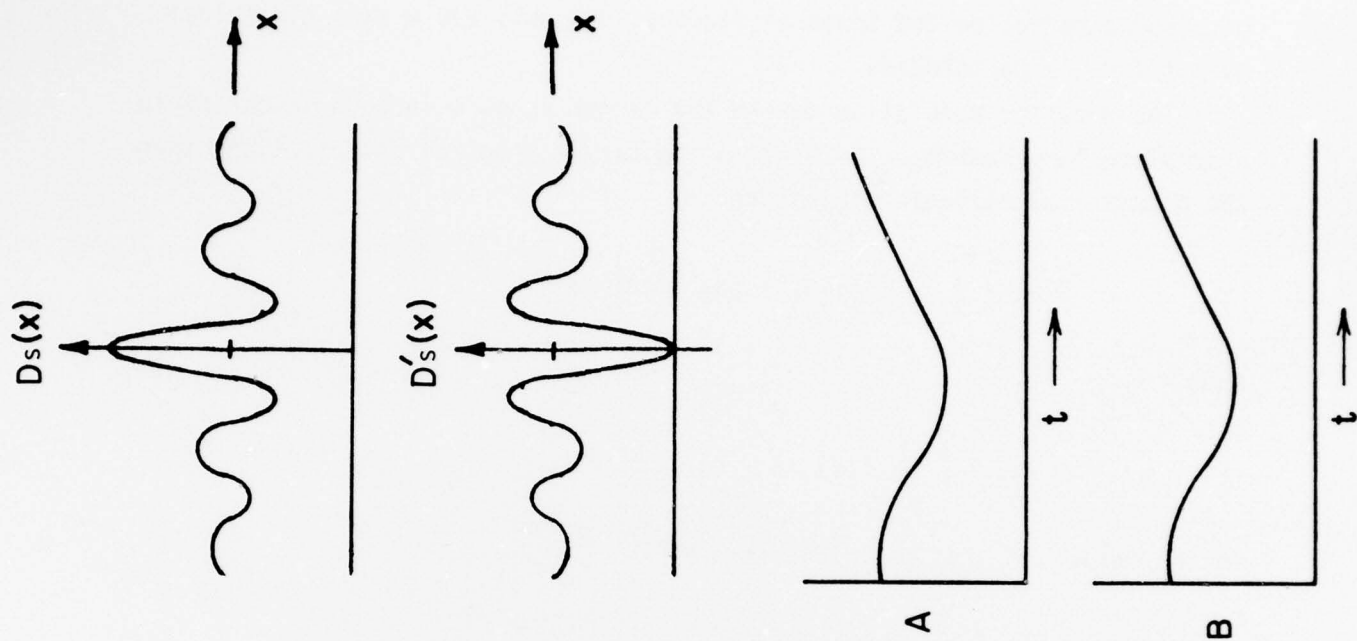


FIGURE 4

Figure 5 shows conceptually the dual-input, dual-output interferometer configuration. In essence what this system accomplishes is to suppress the background radiation and temporal fluctuations to yield a zero electrical output for the background.

The detector modulation due to the target appears in both detectors in a complementary fashion. If $T(\sigma)$ is the target spectral distribution, then the detector electrical outputs are

$$D(x) = \int \frac{1}{2} T(\sigma) [1 + \cos 2\pi\sigma x] d\sigma$$

and

(10)

$$D'(x) = \int \frac{1}{2} T(\sigma) [1 - \cos 2\pi\sigma x] d\sigma,$$

which yields a D_d for the difference of

$$D_d = \int T(\sigma) \cos 2\pi\sigma x d\sigma. \quad (11)$$

This D_d is a target signal which is twice what one would obtain with one detector. However, using two detectors increases the noise by the $\sqrt{2}$, so that the gain in S/N is the $\sqrt{2}$. Thus, the Fig. 5 configuration is capable of background suppression, including intensity fluctuations and yields a gain in S/N of the $\sqrt{2}$.

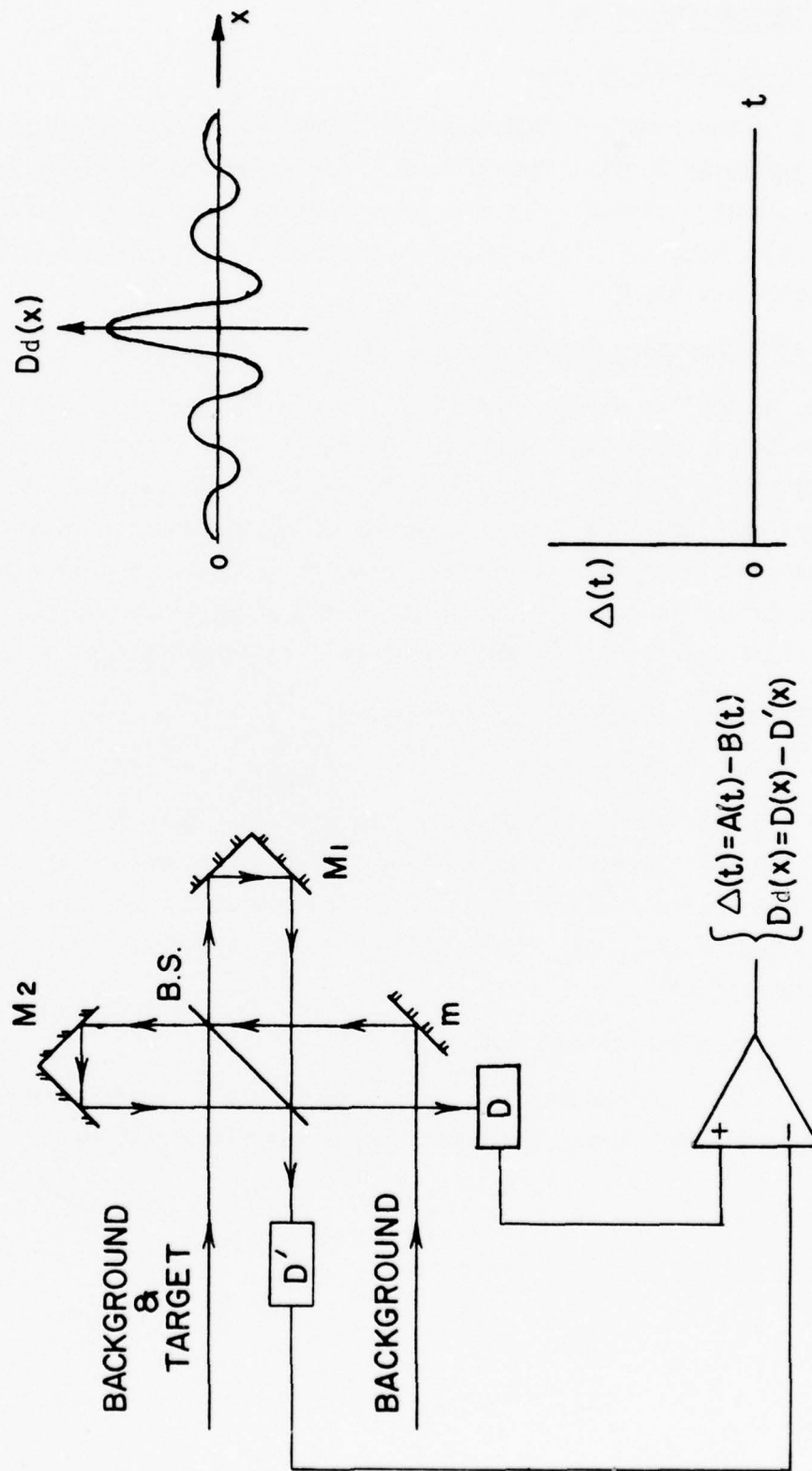


FIGURE 5

3. CONCEPTUAL IMPLEMENTATIONS

A. Adjacent Fields-Of-View

This is the simplest implementation (See Fig. 2) which consists of two adjacent apertures to the interferometer, corresponding to adjacent footprints in the target vicinity. For the interferometer set at zero retardation a positive or negative signal would be generated as the target came within one field-of-view.

B. Multiple Aperture Single Field-Of-View

This concept is illustrated in Figure 6. The system is a cat's eye retroreflector interferometer, where now one field-of-view impinges on a mask consisting of alternate reflecting and transmitting facets. This mask breaks up the background between beams striking the upper face of the beamsplitter and beams striking the lower face, to produce background suppression. The target is mostly either transmitted or reflected by the mask and would generate a positive or negative signal as it goes across the mask.

C. Tailored MTF (Proprietary to Visidyne)*

(i) Two Fields-Of-View

This implementation is illustrated in Figure 7. The principle is the MTF of the two fields-of-view so that the resultant modulation is due only to large spatial frequencies. For a uniform background the result should be as shown in the upper right, while for the target it should be as shown in the lower right.

(ii) Single Field-Of-View

This implementation is shown in Figure 8, where an extra beamsplitter is inserted to produce two beams out of one field-of-view.

*Patent pending

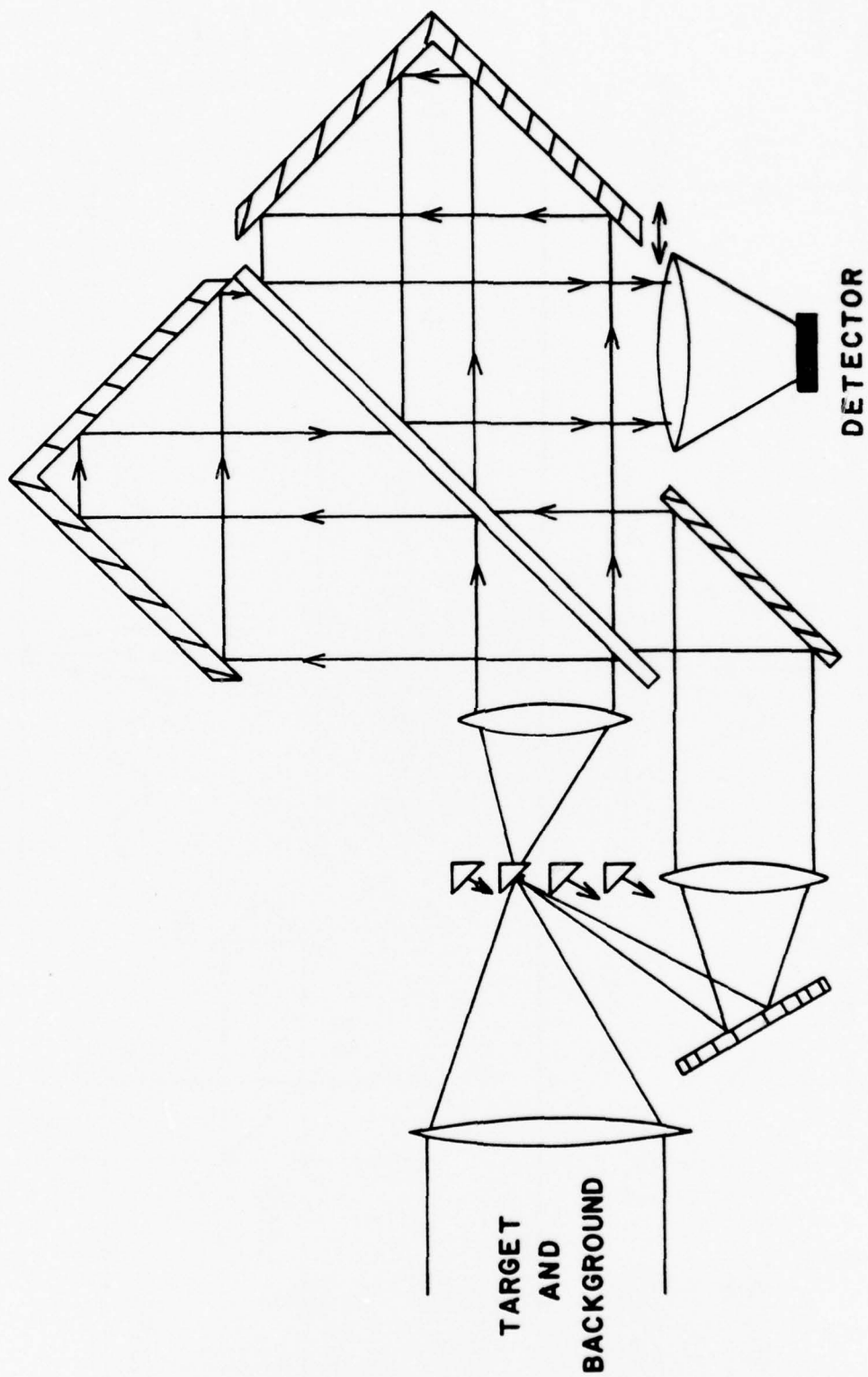
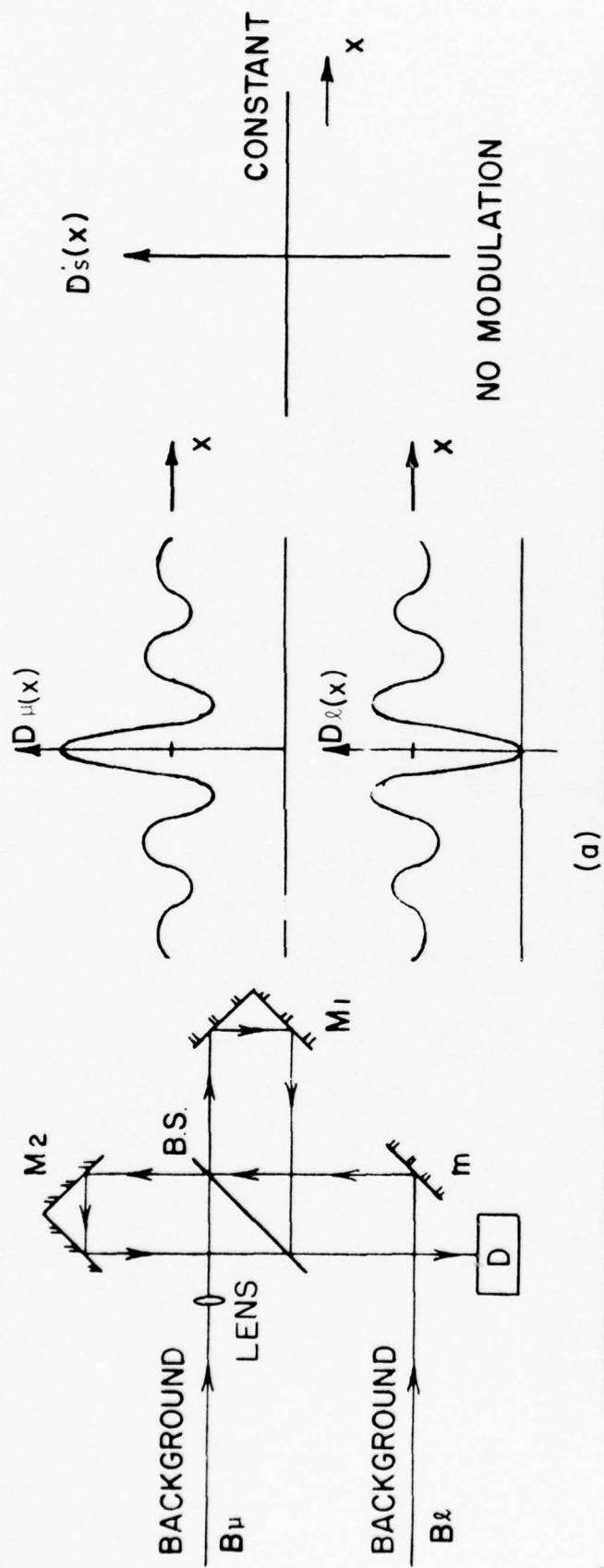
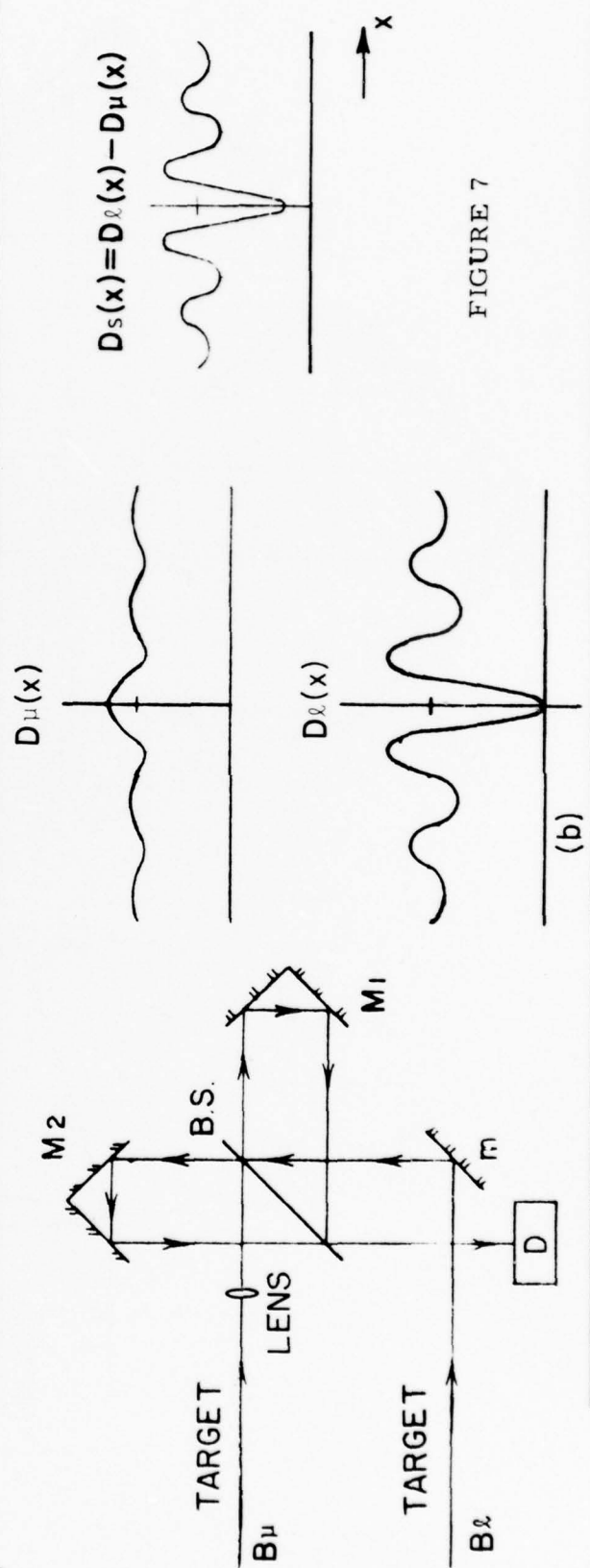


FIGURE 6



(a)



(b)

FIGURE 7

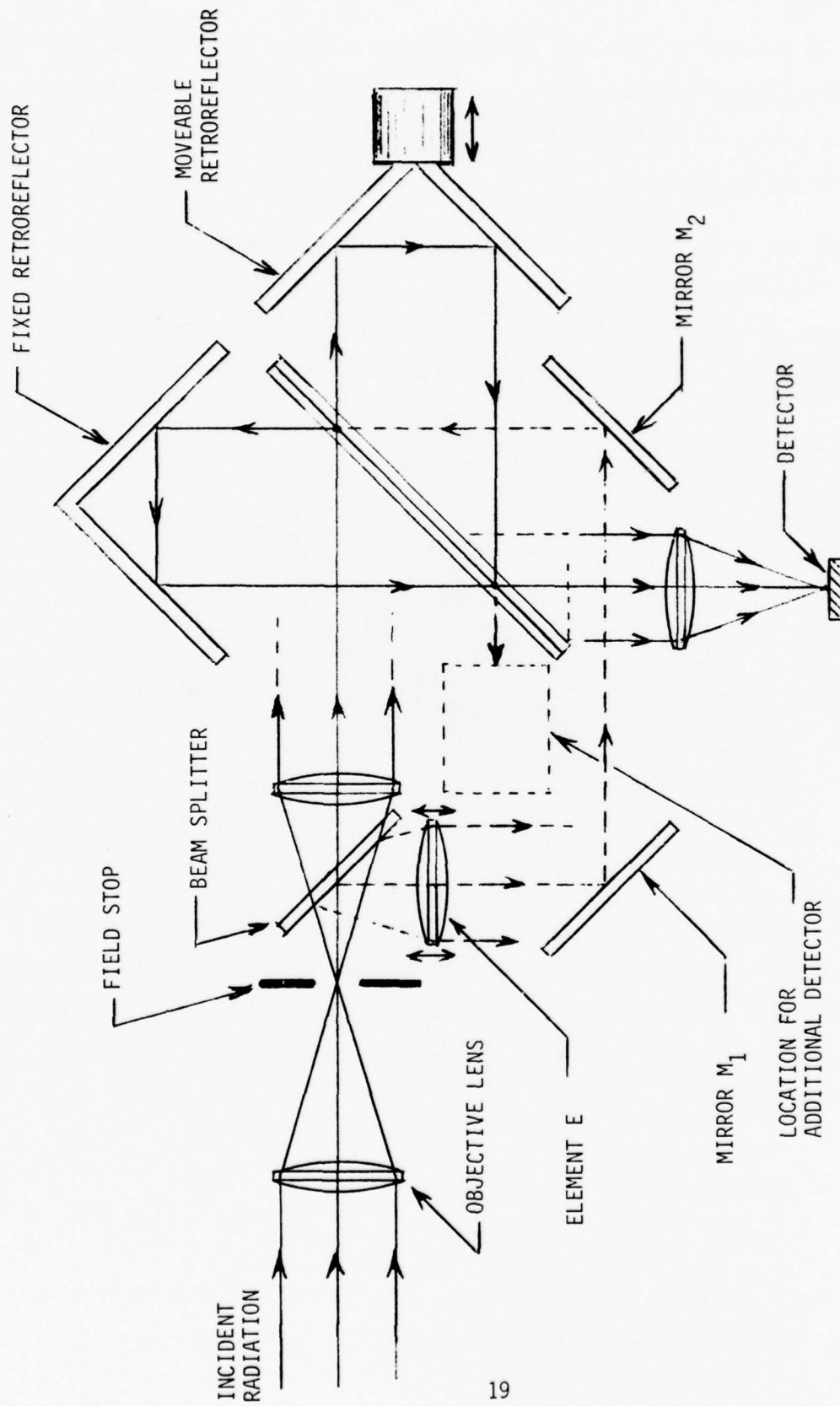
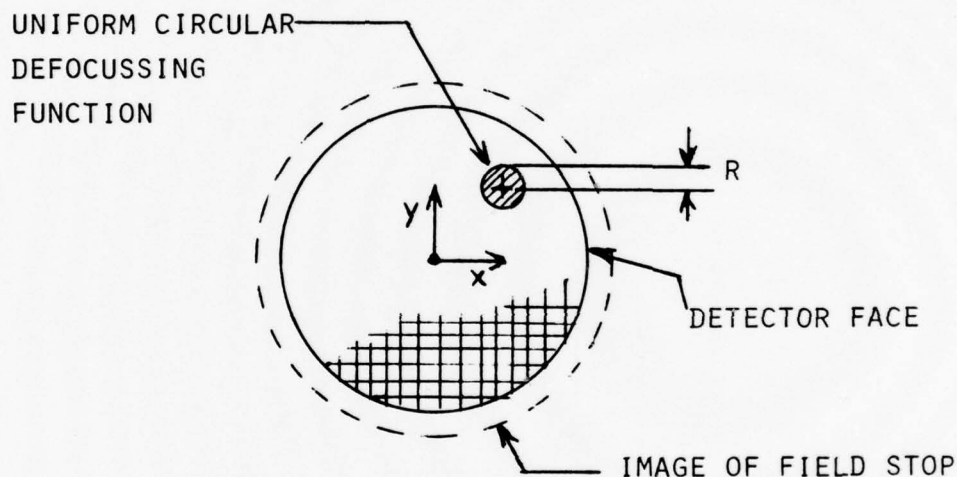


FIGURE 8

D. Suppression of Linearly Varying Background

One method of tailoring the MTF is to slightly defocus the radiation in one arm of the interferometer. In this section, we consider the response of a dual beam interferometer with one arm defocussed to a linearly varying background.

Let the background intensity, if it were to be sharply focussed onto the detector face, be given by the function $B(x, y)$. However, let the image actually be defocussed such that radiation from any point in object space is mapped into a circular area of radius R on the detector face:



To find the intensity distribution $B'(x, y)$ in the defocussed image, the defocussing function must be convolved with the function $B(x, y)$. The contribution to the intensity at some point (x, y) due to the defocussed radiation from some nearby point (X, Y) which is separated from (x, y) by no more than distance R will be:

$$\frac{B(X, Y) dYdX}{\pi R^2}$$

The background intensity $B'(x, y)$ in the defocussed image at (x, y) is then found by integrating over an area A of radius R centered on (x, y) :

$$B'(x, y) = \iint_A \frac{B(X, Y)}{\pi R^2} dY dX$$

$$= \frac{1}{\pi R^2} \int_{X_b}^{X_a} \int_{Y_b}^{Y_a} B(X, Y) dY dX$$

The equation of the boundary of the circular area A is given by:

$$(X - x)^2 + (Y - y)^2 = R^2$$

Therefore, the limits of integration are given by:

$$X_a = x + \sqrt{R^2 - (Y - y)^2}$$

$$X_b = x - \sqrt{R^2 - (Y - y)^2}$$

$$Y_a = y + R$$

$$Y_b = y - R$$

For a sample background function, select the simple case where the background varies linearly across the field of view in the x direction:

$$B(x, y) = Hx + C$$

The values of H and C must be such that B(x, y) is not less than zero for any value of x within the field of view.

$$B'(x, y) = \frac{H}{\pi R^2} \iint_A x dx dy + \frac{C}{\pi R^2} \iint_A dx dy$$

$$= \frac{H}{2\pi R^2} \left[\int_{Y_b}^{Y_a} x^2 dY \right]_{X_b}^{X_a} + \frac{C}{\pi R^2} (\pi R^2)$$

$$B'(x, y) = \frac{H}{2\pi R^2} \int_{Y_b}^{Y_a} \left[\left(x + \sqrt{R^2 - (Y - y)^2} \right)^2 - \left(x - \sqrt{R^2 - (Y - y)^2} \right)^2 \right] dY + C$$

$$= \frac{2Hx}{\pi R^2} \int_{Y_b}^{Y_a} \sqrt{R^2 - (Y - y)^2} dY + C$$

$$= \frac{Hx}{\pi R^2} \left[(Y - y) \sqrt{R^2 - (Y - y)^2} + R^2 \sin^{-1} \left(\frac{Y - y}{R} \right) \right]_{y-R}^{y+R} + C$$

$$= \frac{Hx}{\pi} [\sin^{-1}(1) - \sin^{-1}(-1)] + C$$

$$B'(x, y) = \frac{Hx}{\pi} + C$$

where $\alpha = \dots -5, -3, -1, +1, +3, +5, \dots$

However, the negative values of α can be rejected because, being an intensity, $B'(x,y)$ must be positive. The $+3, +5, \dots$ values can be rejected because energy must be conserved. Thus, $\alpha = +1$ and:

$$B'(x,y) = Hx + C$$

Therefore, for the chosen defocussing function, the focussed and defocussed images are identical for a background which varies linearly across the field of view.

E. Spatially Offset Complementary Beam

This technique is conceptually similar to the defocussed technique. Rather than spreading the target signal over a number of pixels the images in the two channels are offset a fixed amount.

This technique is illustrated in Figure 1b, the two images in the detector plane are offset by one or two pixels (detector resolution element). If the background spatial structure scale is large compared to the target or pixel size, (which is the basic assumption in the discrimination technique) a shift of one or two pixels will be equivalent to a small change or no change in background signal and the background interferograms will be complementary or almost complementary. On the other hand, the target interferogram for one channel will be in a different pixel than for the other channel. The target signal will not be suppressed and significant background discrimination will be achieved.

4. PROBLEM OF NON-UNIFORM BACKGROUND

The Lockheed data show that the Wiener spectrum of the background decreases with increasing spatial frequency. This implies that the fine structure in the background that would tend to degrade the background suppression scheme is of low amplitude.

Figure 9 illustrates the anticipated effect using a tailored MTF. The optimum design is one for which only the high spatial frequency response in the two arms is different. The optical transfer function (OTF) for the two beams should be essentially the same for the low spatial frequencies. Because of this, these should be suppressed in the dual beam mode. The high spatial frequencies will not be so suppressed, but because of the natures of the power spectrum of the background and a point target, the system should show an enhancement for target detection.

5. ADVANTAGES OF THE TECHNIQUE

A. Dynamic Range Reduction

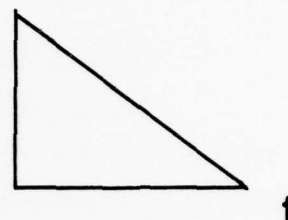
By using two input beams for optical background suppression, the detectors never see the large central peak in the interferogram due to background radiation. If there occurs a dynamic range problem it's because the target is too bright.

B. Work With Unknown Spectral Distributions

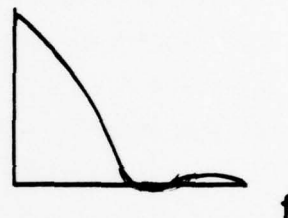
It is not necessary that the target spectral signatures be uncorrelated with the background spectral distribution. In fact, the background could radiate a sharp line at the same wavelength as the target, and it will still be suppressed.

SPATIAL FREQUENCY PERFORMANCE OF THE TAILORED DBI

A) OTF OF ARM 1
(A)



B) OTF OF ARM 2
(B)



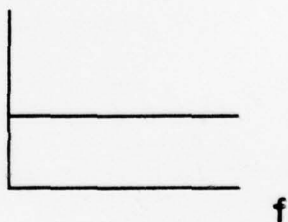
C) OTF OF DBI
(A-B)



D) POWER SPECTRUM OF A TYPICAL
NATURAL BACKGROUND



E) POWER SPECTRUM OF A
POINT SOURCE TARGET



F) TARGET/BACKGROUND S/N



FIGURE 9

C. Automatic Background Suppression

If the system views a changing background, whether spatially, temporally, or spectrally (as might happen for a scanning system, or for a staring system which drifts) the background suppression scheme will still be effective.

D. Capability of Making Use of Known Signatures

For example, if it is known that a target emits lines which are equally, or about equally spaced, then the system can preferentially modulate the target energy versus the background. This is in addition to the background suppression which is always being done. If the lines happen to have spacing $\Delta\sigma$ equal to 1 cm^{-1} , then the interferometer is placed at a retardation X of $1/2 \Delta\sigma = 1 \text{ cm}$. At the retardation the transmission function for the interferometer peaks at exactly where the target line emissions occur. If the retardation is made to oscillate about this 1 cm position, then the target radiation is chopped, but not the background radiation.

E. Insensitive to Multiplicative Noise

As described above, using the two outputs in an electronic differencing mode compensates for apparent or actual temporal fluctuations of the background.

6. OTHER CAPABILITIES

- Obtain target velocity

- Obtain target extent

- Works as well in occultation mode

- Can work as detection, discrimination scheme

- Obtain target signatures covering large spectral band

- Obtain background target signatures in single-input mode

- Interferometer can be field-widened

Electronic filtering can be accomplished by tuning to the retardation jitter frequency bandpass. Jitter period could be done about $1/5$ to $1/10$ the time it takes the target to move across the field-of-view; larger size objects would produce much lower frequencies.

In dual input only approach of adjacent fields-of-view the focal plane fill factor could be reduced by two.

7. LABORATORY MEASUREMENTS OF BACKGROUND SUPPRESSION

INSTRUMENTATION

A Michelson interferometer, using roof mirrors instead of plane mirrors, was designed and assembled, and is shown in Figure 10. Specifications are given below.

Interferometer

Beamsplitter	Idealab CaF_2
Drive	Motor-driven X-Y-Z Translator
Mirror Type	Roof Retroreflector
Detector Lens	CaF_2 f/2
Spectral Range	2.1 to 2.5 μm
Field-of-View	0.2 degrees
Aperture	3.2 mm dia
Detector	Pbs

Test Source

Tungsten-Halogen Lamp ($\sim 3000^\circ \text{K}$)
Opal Diffuser
12.5 inch-f/8-Au Coated Parabolic Collimator

This breadboard instrumentation was designed to permit the use of both Roof and corner cube retroreflectors. Detectors were located in each of the two output beams and a differencing electronics were provided so as to have double input/double output operation.

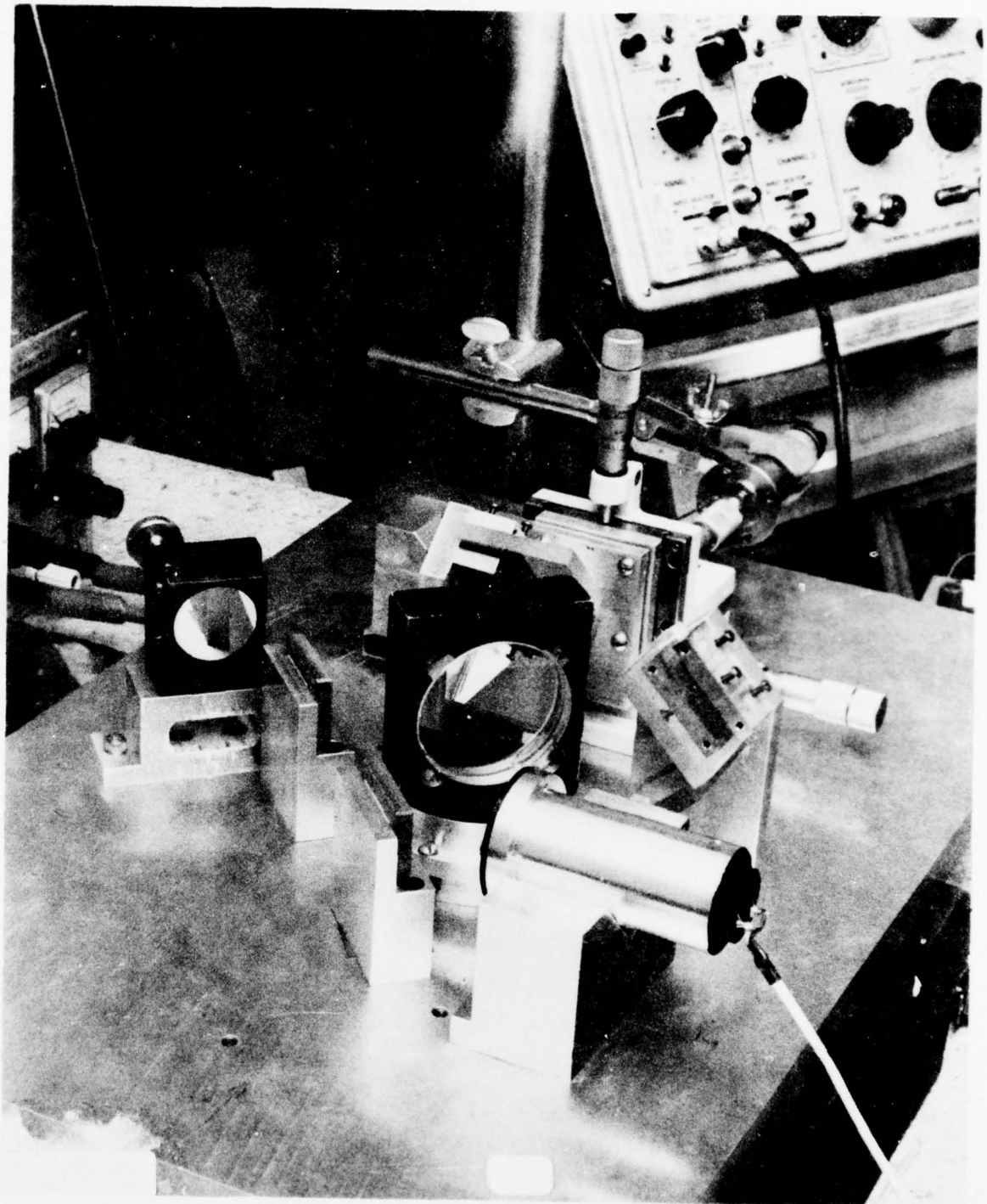


FIGURE 10

NON-UNIFORM BACKGROUND

Figure 11 is a spatial scan of the extended source used for the background suppression measurements presented in this section and in Section 8. Figure 11 and the data presented in this report indicate that this background suppression technique is effective against non-uniform backgrounds.

BACKGROUND SUPPRESSION

The system was tested in the dual-input mode for its background suppression capability, and Figure 12 illustrates the results. The upper left trace of Figure 12 shows a background interferogram due to one beam only, while the upper right trace is the interferogram obtained from the other beam only. The lower left trace shows the resultant interferogram when both background beams enter the interferometer simultaneously; the modulation is practically all gone. The lower right trace is again the dual-input beam interferogram with a gain change of 20. The large periodic oscillations that can be seen are due to source fluctuations. At the time of measurement no other detector was available for differencing the two output beams. The suppression ratio R is defined

$$R = \frac{A(x) - B(x)}{\Sigma(x)}$$

where

$A(x)$ = Single Beam Background Interferogram

$B(x)$ = Single Beam Complementary Background Interferometer

$\Sigma(x)$ = Double Beam Background Interferogram
= $A(x) + B(x)$

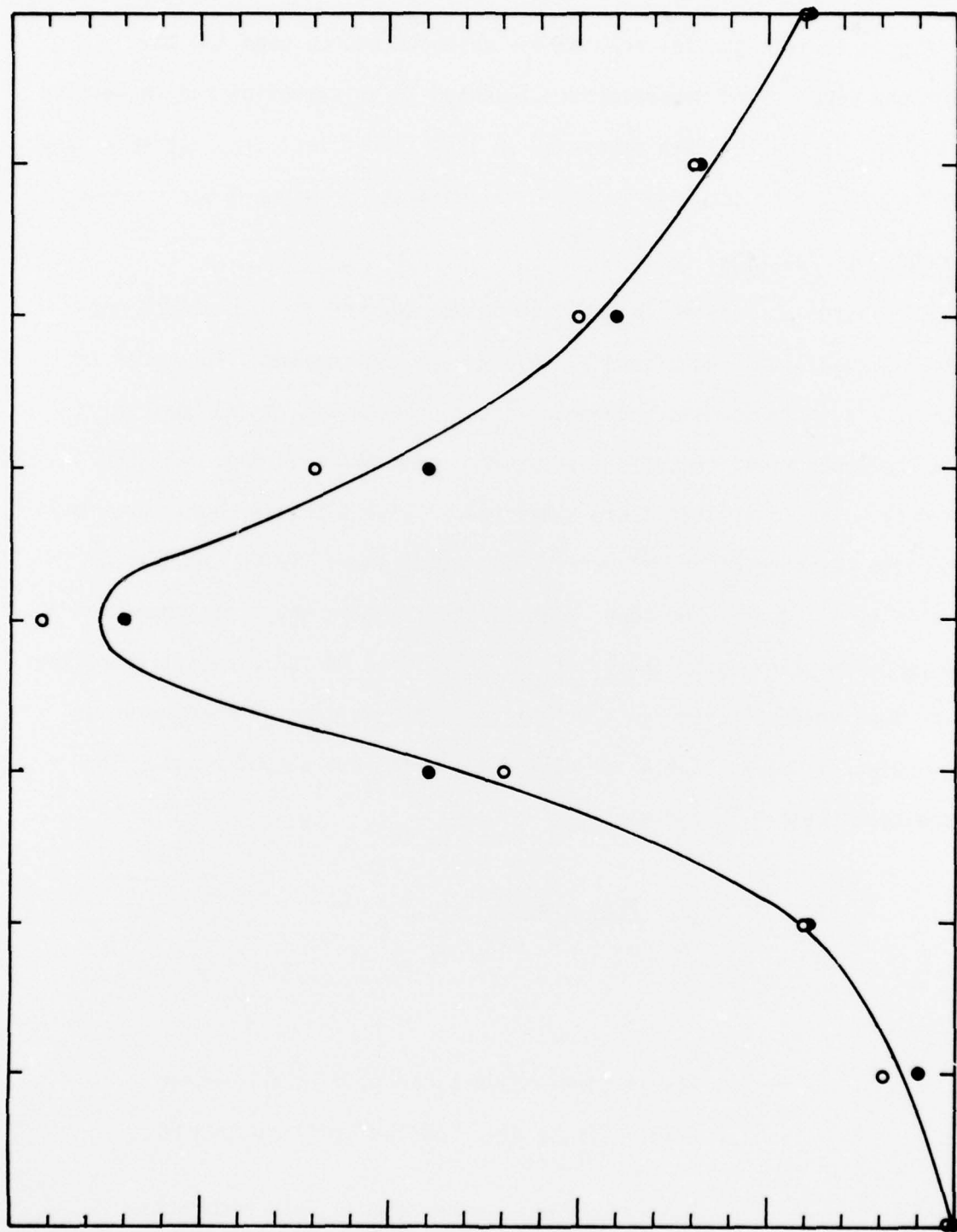
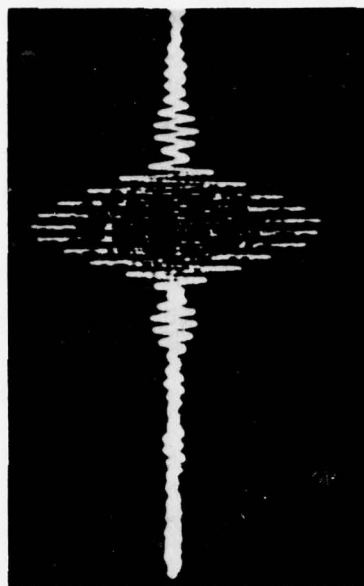


FIGURE 11

DOUBLE-BEAM INTERFEROMETER LABORATORY TEST RESULTS



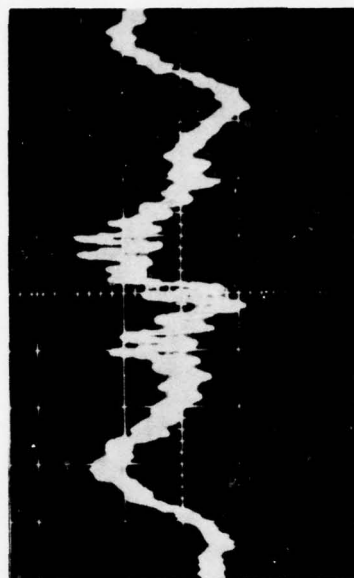
SINGLE-BEAM BACKGROUND
INTERFEROGRAM



SINGLE-BEAM COMPLEMENTARY
BACKGROUND INTERFEROGRAM



DOUBLE-BEAM BACKGROUND
INTERFEROGRAM



DOUBLE-BEAM BACKGROUND
INTERFEROGRAM (20X GAIN)

FIGURE 12

Evaluating R for the results given in Figure 2 (and neglecting the non-interferometric modulation yields:

$$R \approx 200$$

8. LABORATORY MEASUREMENTS OF BACKGROUND SUPPRESSION WITH OCCULATION

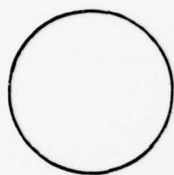
The two beams of the double-beam interferometer were spatially displaced, as shown in Figure 13(b) so that each viewed a different region of the background. The background interferogram of Figure 13(a) was obtained when only a single-beam was viewing the background. Since the source was uniform over both fields-of-view, the background suppression of Figure 13(b) was observed. With the interferogram operating in this displaced field-double-beam mode, a simulated target at infinity was positioned in one of the fields-of-view. The observed target interferogram is seen in Figure 13(c). Because of the simulated target used for this test did not emit any radiation, but occulted some of the background, the target interferogram is that of the background radiation obscured by the target.

9. LABORATORY MEASUREMENTS OPTICAL TARGET FILTERING

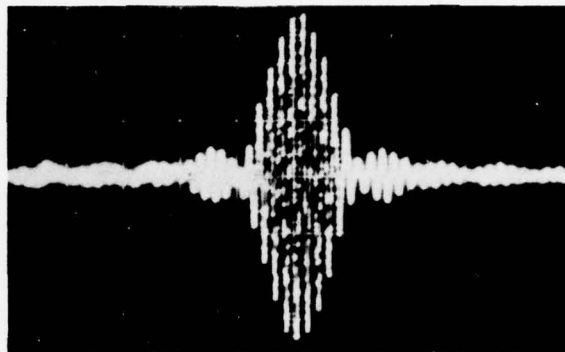
The laboratory breadboard instrument shown in Figure 10 was utilized for these measurements; the layout is shown schematically in Figure 14 and the two inputs of the interferometer viewed the identical scene which was presented at infinity. Figures 15, 16, and 17 show laboratory data demonstrating background suppression using optical defocussing. In Figures 15,

DOUBLE-BEAM INTERFEROMETER
LABORATORY TARGET DETECTION

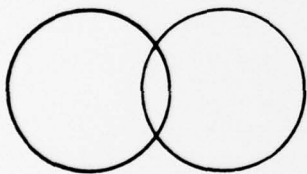
SINGLE-BEAM INTERFEROGRAM
OF BACKGROUND



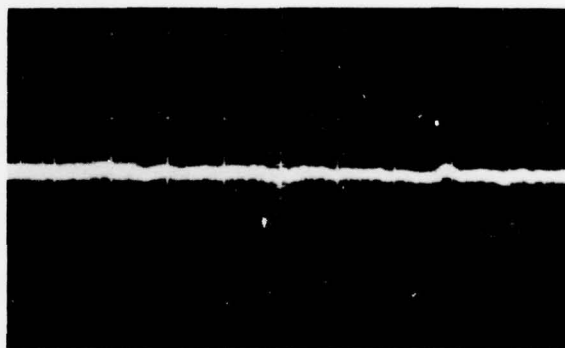
(A)



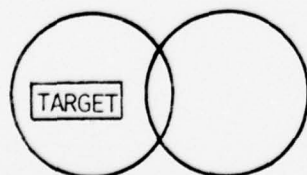
DOUBLE-BEAM INTERFEROGRAM
OF BACKGROUND WITH
DISPLACED FIELDS OF VIEW



(B)



DOUBLE-BEAM INTERFEROGRAM
OF BACKGROUND PLUS TARGET
WITH DISPLACED FIELDS OF VIEW



(C)

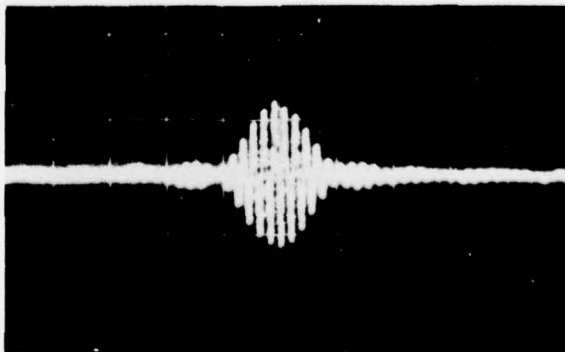


FIGURE 13

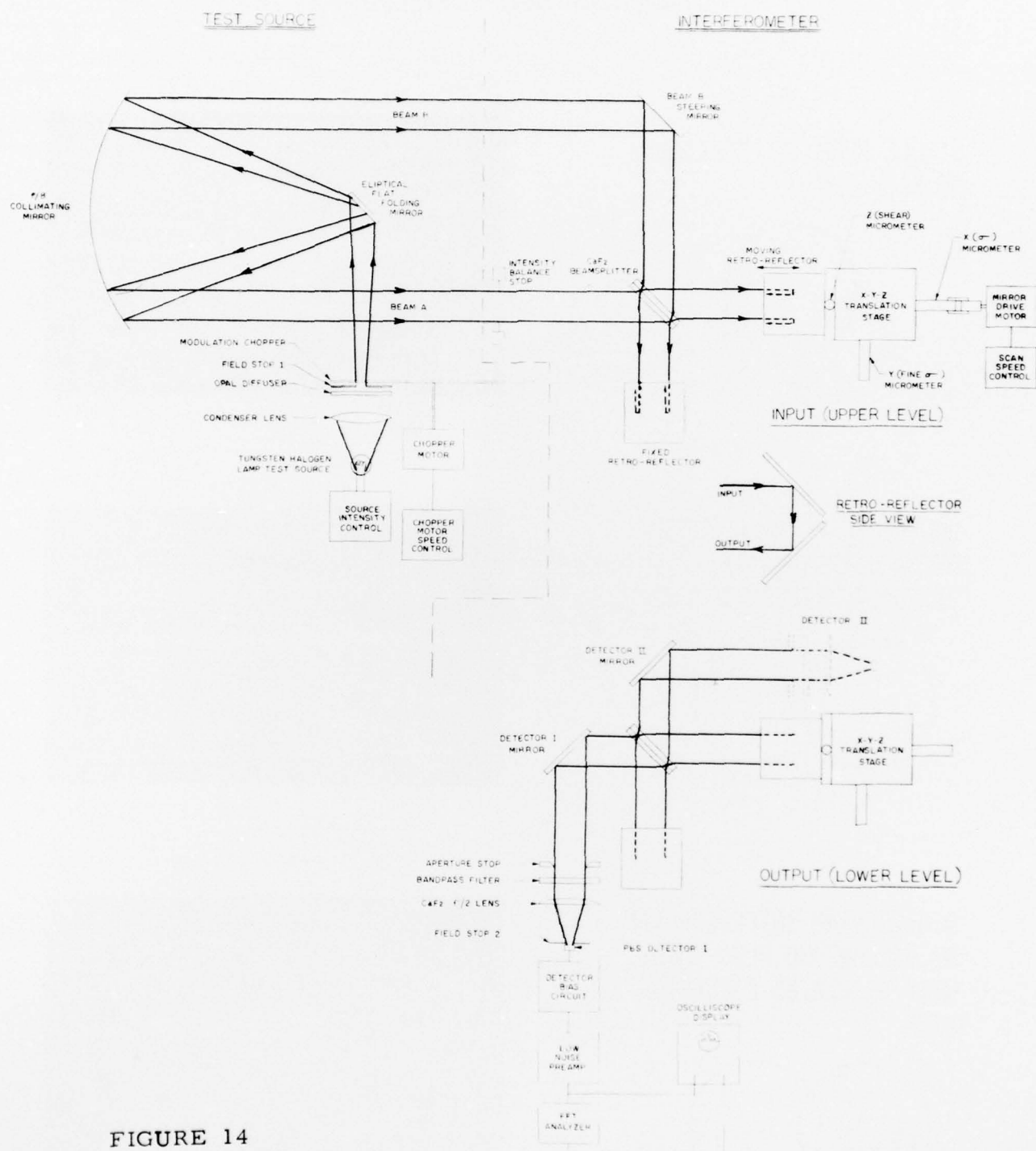
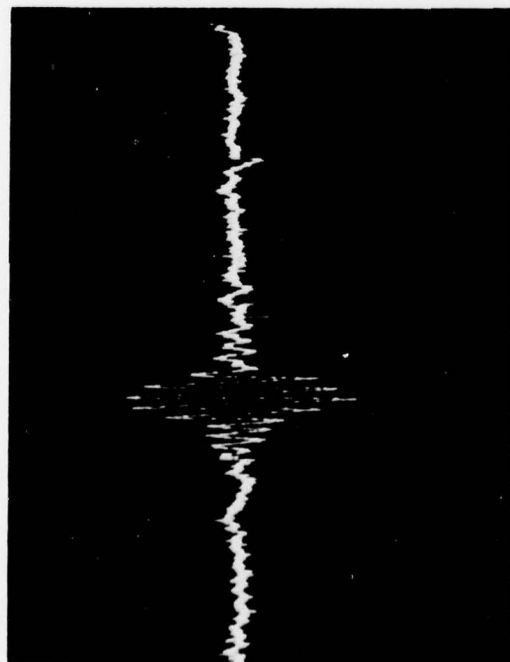


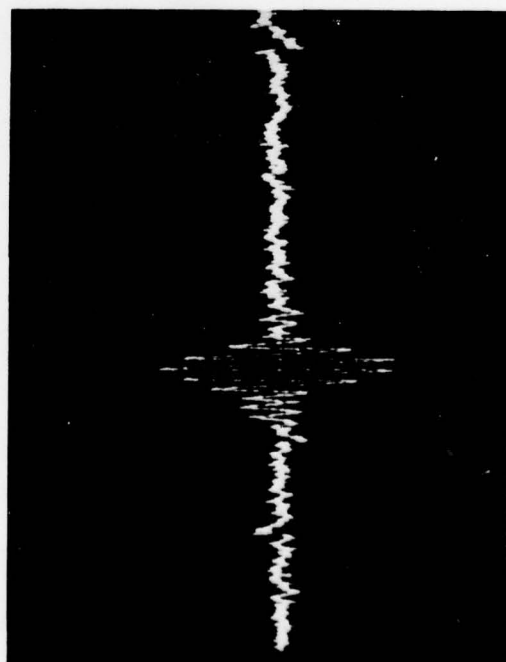
FIGURE 14

BACKGROUND OPTICAL SUPPRESSION SYSTEM
LABORATORY DATA
DEFOCUSED DOUBLE BEAM INTERFEROMETER
SPATIALLY EXTENDED BACKGROUND SOURCE



SINGLE BEAM
INTERFEROGRAM

BEAM A



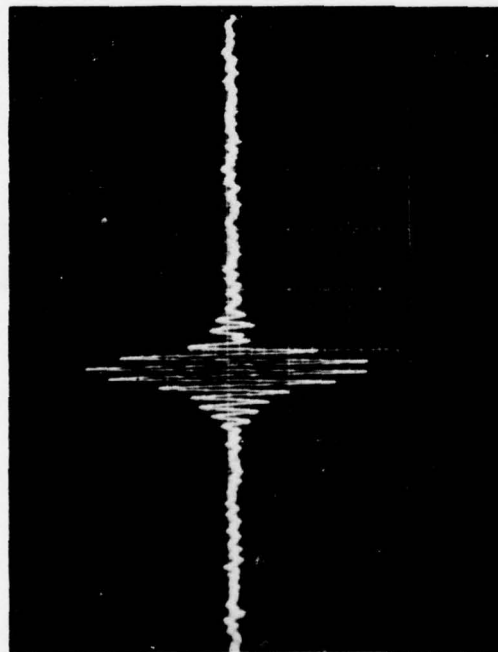
BEAM B



DOUBLE BEAM INTERFEROGRAM

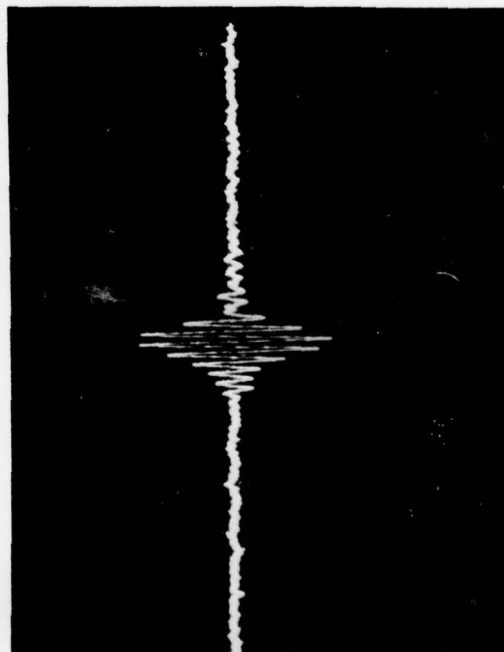
FIGURE 15

BACKGROUND OPTICAL SUPPRESSION SYSTEM
LABORATORY DATA
DEFOCUSED DOUBLE BEAM INTERFEROMETER
POINT SOURCE (SIMULATED TARGET)

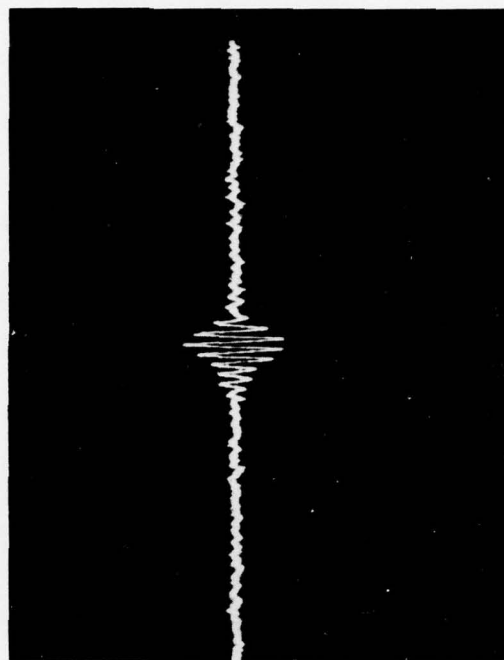


SINGLE BEAM
INTERFEROGRAMS

BEAM A



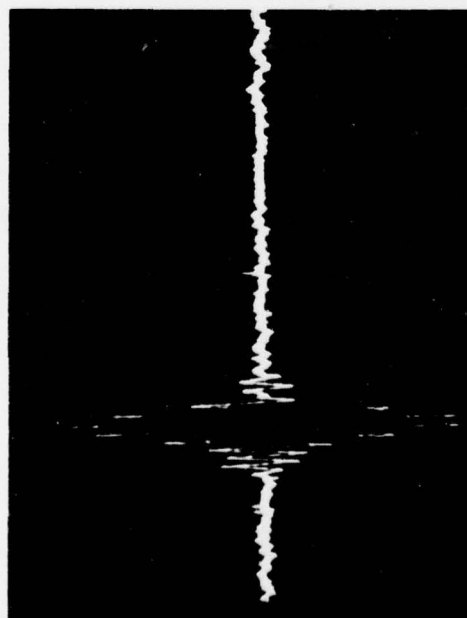
BEAM B
(DEFOCUSED)



DOUBLE BEAM INTERFEROGRAM

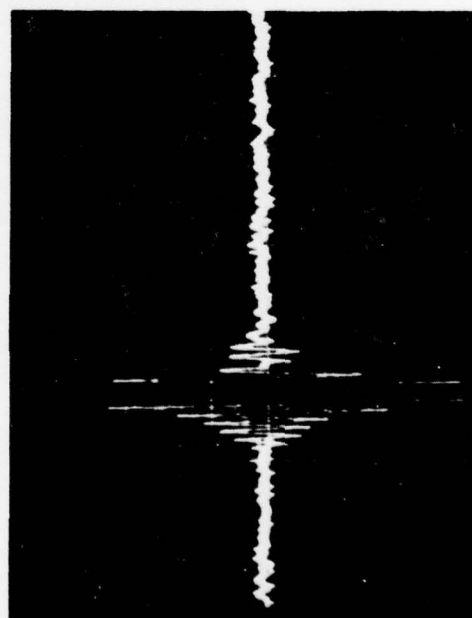
FIGURE 16

BACKGROUND OPTICAL SUPPRESSION SYSTEM
LABORATORY DATA
DEFOCUSSED DOUBLE BEAM INTERFEROMETER
POINT SOURCE (SIMULATED TARGET) PLUS SPATIALLY EXTENDED BACKGROUND

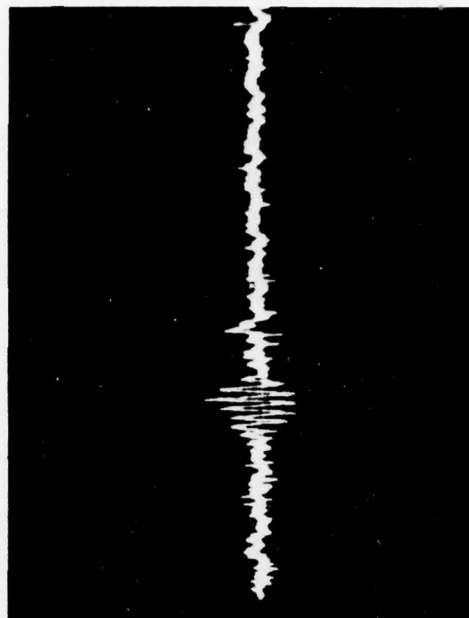


SINGLE
BEAM INTER-
FEROGRAM

BEAM A



BEAM B



DOUBLE BEAM INTERFEROGRAM

FIGURE 17

16, and 17 Beam B was defocussed. Beam A was not. As the photographs on the right show the interferometer output with only one input, the photograph on the left is the output with dual input (both beams simultaneously). In Figure 15, the scene viewed was a spatially extended background. As anticipated, the focussed and defocussed single beam outputs are essentially identical and background suppression is essentially complete. In Figure 16, the interferometer is looking at a point source. The power in the defocussed (Beam B) interferogram is appreciably decreased. The reduction in power is a function of the experiment set-up (detector size, degree of defocussing). No attempt was made in these measurements to optimize the power reduction. Again, as anticipated, the unbalanced interferograms, in the dual beam mode do not cancel, but produce a net interferogram.

As a final demonstration of the technique, measurements were made at the same power levels of the scene containing both the point source and the extended background. (Figure 16). In the single beam mode, the interferogram is dominated by the background spectrum and there is no obvious difference between the focussed and the defocussed beams. However, in the dual beam mode, the background is suppressed and the resulting interferogram is essentially identical to that of the target alone (Figure 16).

10. PRESENT STATUS AND FUTURE WORK

This effort:

- (1) has demonstrated that the dual beam spectrometer technique can suppress the amplitude of the interferogram of a non-uniform background by a factor of 200; and
- (2) has shown that the dual beam technique is effective both in the occultation and the emission mode.

Further laboratory work is necessary to determine the achievable suppression using laboratory sources simulating real data for targets and background. Specifically it is proposed (1) to use the Lockheed data as a model for the background spatial frequency distribution; (2) to use AFGL (OP) data and transmission models for the spectral distribution of sources and background, specifically in the 2.7 and 4.3 band blue and red spikes; and (3) to develop an improved laboratory instrument with the capability of

- a. Optically balancing the two arms of the interferometer to obtain maximum suppression
- b. using optical techniques other than defocussing to tailor the MTF
- c. using two output detectors simultaneously to suppress temporal fluctuations
- d. proving the capability of near real time transformation from interferogram to spectrum.